J. Chem. Eng. Data 1990, 35, 127-130

Acknowledgment

We thank Jan Chipperfield for her assistance in collecting the data.

Glossary

$C_{L,l}$	liquid-phase concentration (at time l) (mol L^{-1})
H	solubility coefficients (MPa L mol^{-1})
k_La	mass-transfer coefficient (s^{-1})
N	number of moles (mol)
P	pressure (MPa)
R	gas constant
t	time (s)
T	temperature (K)

Subscripts

V	volume (L)
0	time = 0
eq	equilibrium

Registry No. H_2, 1333-74-0; CO, 630-08-0; *n*-octacosane, 630-02-4.

Literature Cited

(1) Ledakowiscz, S.; Nettlehof, H.; Deckwer, W.-D. *Ind. Eng. Chem. Fundam.* **1984**, *23*, 510.
(2) Albal, R. S.; Shah, Y. T.; Carr, N. L.; Bell, A. T. *Chem. Eng. Sci.* **1984**, *39*, 905.
(3) Karandikar, B. M. An experimental study of gas liquid mass transfer at Fischer-Tropsch reaction conditions. Ph.D. Thesis, University of Pittsburgh, 1986.
(4) Huang, S. H.; Lin, H. M.; Tsai, F. N.; Chao, K. C. *Ind. Eng. Chem. Res.* **1988**, *27*, 162.
(5) Karandikar, B. M.; Morsi, B. I.; Shah, Y. T.; Carr, N. L. *Chem. Eng. J.* **1986**, *33*, 157.
(6) Karandikar, B. M.; Morsi, B. I.; Shah, Y. T.; Carr, N. L. *Can. J. Chem. Eng.* **1987**, *65*, 973.
(7) Miller, S. A.; Ekstrom, A. Unpublished work.
(8) Kuo, J. C. W. Slurry Fischer-Tropsch/Mobil two stage process of converting syngas to high octane gasoline. Final Report, DOE/PC/30022-10, 1983.

Received for review February 28, 1989. Accepted December 6, 1989. This work was supported by a CSIRO/UNSW Collaborative Research Fund.

Viscosity Behavior of Potassium Iodide in *N*-Formylmorpholine Solutions at Several Temperatures

Souad F. Al-Azzawi* and Muna A. Salman

Petroleum Research Centre, Jadiriyah, P.O. Box 10039, Baghdad, Iraq

The viscosity of potassium iodide in *N*-formylmorpholine was measured at 25, 35, 45, and 55 °C in a range of 0–1.0 M composition. The viscosity shows a negative deviation over the whole composition range and all the temperatures studied. The activation energies of viscous flow were calculated, and their significance is discussed. The ionic *B* coefficients have been determined at low concentrations and interpreted qualitatively.

Introduction

Ion–solvent interactions have been studied extensively in aqueous solution (*1–4*). Less attention has been given to such interactions in nonaqueous solvents. Therefore, we have initiated a program to study ion–solvent interactions of salts in highly dense, highly polar, and highly selective solvents for the extraction of monocyclic aromatic hydrocarbons, such as *N*-formylmorpholine (*5*), ethylene glycol (*6*), and *N*-methylpyrrolidone (*7*). These solvents readily dissolve potassium iodide. As a first part of this work, we have measured the densities and viscosities of potassium iodide in *N*-formylmorpholine in the range of 0–1.0 M and at 25, 35, 45, and 55 °C. The Jones and Dole (*8*) empirical equation has been used for determining viscosity *B* coefficients at low concentrations.

Experimental Section

Materials. *N*-Formylmorpholine (NFM), Puriss Grade (Fluka AG), was used without further purification, kept over an activated molecular sieve of type 4A (Union Carbide) for 2 days, and filtered before use. The purity was checked by GLC and was found to be >99.5 mol %.

Potassium iodide (KI), Chemically Pure (Riedel-de Haen AG), was dried for 24 h at 110 °C prior to use and stored over P_2O_5 in a glass desiccator.

Densities Measurements. Densities were determined with an Anton Paar (Model DMA 602) digital densimeter, thermostated to ±0.01 °C. The overall precision of the densities is estimated to be better than $\pm 2 \times 10^{-6}$ g cm^{-3} for 25, 35, and 45 °C and $\pm 4 \times 10^{-5}$ g cm^{-3} for 55 °C.

Viscosity Measurements. Viscosities were determined with a suspended-level Ubbelohde viscometer. The flow times were determined electronically with an electronic timer of precision ±0.01 s, and the temperature of the bath was controlled to be better than ±0.01 °C. Viscosities of all solutions were reproducible within ±0.5% at all temperatures studied.

Preparation of Salt Solutions. Solutions were made up by weight with use of a four-place digital balance. Stock solutions of the KI in NFM were prepared by direct weighing, and these were diluted accurately by using previously calibrated glassware to obtain different required concentrations.

Results and Discussion

The obtained densities, viscosities, and refractive indices of solutions of KI in NFM at 25, 35, 45, and 55 °C are listed in Table I. The viscosity increases with decreasing temperature and with increasing molar concentration of KI, Figure 1.

The experimental data were analyzed for low molar concentrations of KI in NFM according to the Jones–Dole equation (*8*)

$$(\eta/\eta_0 - 1)/C^{1/2} = A + BC^{1/2} \qquad (1)$$

where η and η_0 are the viscosities of the solution and pure solvent, respectively; *A* and *B* are the characteristic parameters for salt and solvent, dependent on ion–ion and ion–solvent interactions, respectively; and *C* is the molar concentration of KI in NFM. Plotting $(\eta/\eta_0 - 1)/C^{1/2}$ against $C^{1/2}$ at 25, 35, 45, and 55 °C yields an exponentially increasing function, Figure 2a–d.

0021-9568/90/1735-0127$02.50/0

Table I. Densities, ρ, and Viscosities, η, of KI in NFM at Different Temperatures

C/ (mol L^{-1})	ρ/ (g cm^{-3})	η/cP	C/ (mol L^{-1})	ρ/ (g cm^{-3})	η/cP
		At 25 °C			
0.00	1.1463	7.827	0.20	1.1699	10.929
0.01	1.1476	8.031	0.30	1.1822	12.815
0.02	1.1488	8.205	0.40	1.1936	15.158
0.03	1.1500	8.395	0.50	1.2058	17.656
0.04	1.1513	8.525	0.60	1.2173	20.990
0.05	1.1523	8.655	0.70	1.2289	24.728
0.06	1.1537	8.835	0.80	1.2395	29.238
0.07	1.1549	8.994	0.90	1.2507	33.750
0.08	1.1563	9.140	1.00	1.2631	38.785
0.10	1.1588	9.441			
		At 35 °C			
0.00	1.1371	5.917	0.40	1.1858	10.496
0.02	1.1397	5.998	0.50	1.1970	11.990
0.04	1.1420	6.143	0.60	1.2087	14.016
0.06	1.1441	6.316	0.70	1.2201	15.918
0.08	1.1463	6.458	0.80	1.2313	18.781
0.10	1.1502	6.664	0.90	1.2426	21.435
0.20	1.1616	7.719	1.00	1.2550	24.555
0.30	1.1735	9.045			
		At 45 °C			
0.00	1.1287	4.513	0.40	1.1770	7.653
0.02	1.1310	4.604	0.50	1.1884	8.752
0.04	1.1334	4.719	0.60	1.2000	9.967
0.06	1.1355	4.833	0.70	1.2112	11.314
0.08	1.1376	4.945	0.80	1.2223	12.788
0.10	1.1412	5.064	0.90	1.2339	14.597
0.20	1.1529	5.772	1.00	1.2461	16.246
0.30	1.1649	6.700			
		At 55 °C			
0.00	1.1200	3.569	0.40	1.1682	5.795
0.02	1.1220	3.648	0.50	1.1794	6.500
0.04	1.1244	3.735	0.60	1.1911	7.250
0.06	1.1265	3.814	0.70	1.2018	8.117
0.08	1.1283	3.887	0.80	1.2135	9.122
0.10	1.1325	3.979	0.90	1.2248	10.317
0.20	1.1441	4.507	1.00	1.2373	11.330
0.30	1.1560	5.161			

Table II. Variables for Jones–Dole Plots for KI in NFM at Different Temperatures and Different Solvents

solvent	B coefficient	T/°C
NFM	1.778[a]	25
	1.700[a]	35
	1.384[a]	45
	1.149[a]	55
DMSO	0.815[b]	25
HMPT	1.47[c]	25
MeOH	0.695[d]	25
EG	0.0327[e]	25

[a] This work. [b] Reference 9. [c] Reference 10. [d] Reference 11. [e] Reference 12.

However, in low molar concentrations of KI in the NFM region 0–0.4 M, a straight line is obtained. The Jones–Dole parameters A and B were derived by fitting the experimental data to eq 1. Table II gives the B coefficient of KI in NFM together with the values published in the literature in different solvents (*4*, *10*, *11*).

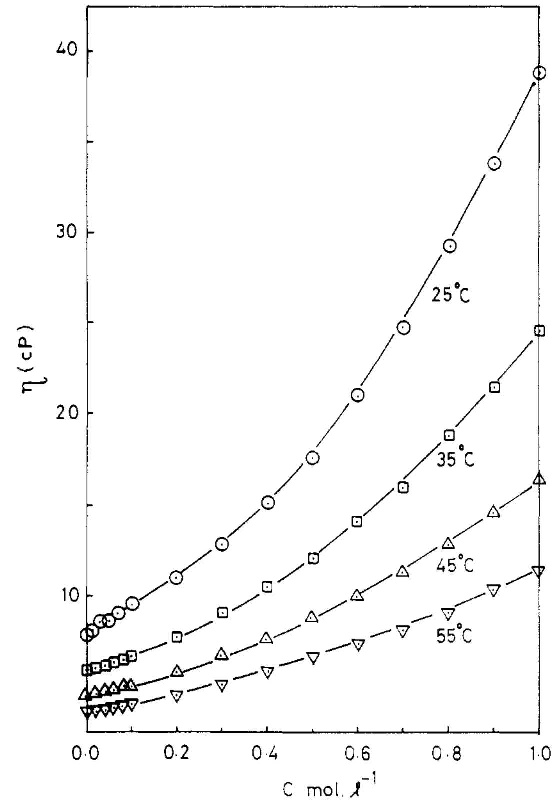

Figure 1. Plots of the viscosity, η (cP), versus the molar concentration, C, of KI in NFM solutions at the temperatures 25, 35, 45, and 55 °C.

The B coefficient values depend on the molar volume of the solvent and the free energy of viscous flow of the solvent, according to the equation (*13*)

$$B = \frac{\bar{V}_1{}^\circ - \bar{V}_2{}^\circ}{1000} + \frac{\bar{V}_1{}^\circ}{1000}\,\frac{(\Delta\mu_2{}^{\circ\ddagger} - \Delta\mu_1{}^{\circ\ddagger})}{RT} \qquad (2)$$

where $\bar{V}_1{}^\circ$ and $\bar{V}_2{}^\circ$ are the partial molar volume of the solvent and solute, respectively; $\Delta\mu_2{}^{\circ\ddagger}$ is the contribution per mole of solute to the free energy of activation for the viscous flow of the solution; and $\Delta\mu_1{}^{\circ\ddagger}$ is the free energy of activation per mole of the pure solvent given by the equation (*14*)

$$\Delta\mu_1{}^{\circ\ddagger} = RT \ln\,(\eta_0\bar{V}^\circ/hN) \qquad (3)$$

In eq 2, the first term is proportional to the molar volume of the solvent and is much smaller than the second term. The calculated contributions of the terms in eq 2 to the B coefficient for the solutions of KI in NFM at 25, 35, 45, and 55 °C are listed in Table III.

The coefficient B has two contributions: one is negative and the other is positive. The positive contribution comes from the tendency of the KI to attract the NFM molecule around it centrosymmetrically while the negative contribution comes from the fact that the structure of the solvent NFM itself goes against this tendency, so that these two opposing influences can cause a breakdown in the NFM structure beyond the solvation shell. Table III shows the positive contribution prevails over the

Table III. Contributions of the Terms of Equation 2 to B Coefficient for KI in NFM Solutions at Different Temperatures

temp/°C	$(\bar{V}_1{}^\circ - \bar{V}_2{}^\circ)/1000$	$(\bar{V}_1{}^\circ/1000) \times [(\Delta\mu_2{}^{\circ\ddagger} - \Delta\mu_1{}^{\circ\ddagger})/RT]$	B	$\Delta\mu_2{}^{\circ\ddagger} - \Delta\mu_1{}^{\circ\ddagger}$/ (kJ mol^{-1})	$\Delta\mu_2{}^{\circ\ddagger}$/ (kJ/mol^{-1})
25	-4.367	6.145	1.778	151.67	135.91
35	-5.504	7.204	1.700	182.30	166.54
45	-5.646	7.030	1.384	182.30	166.54
55	-5.718	6.868	1.149	182.30	166.54

[a] $\Delta\mu_1{}^{\circ\ddagger} = 5.77$.

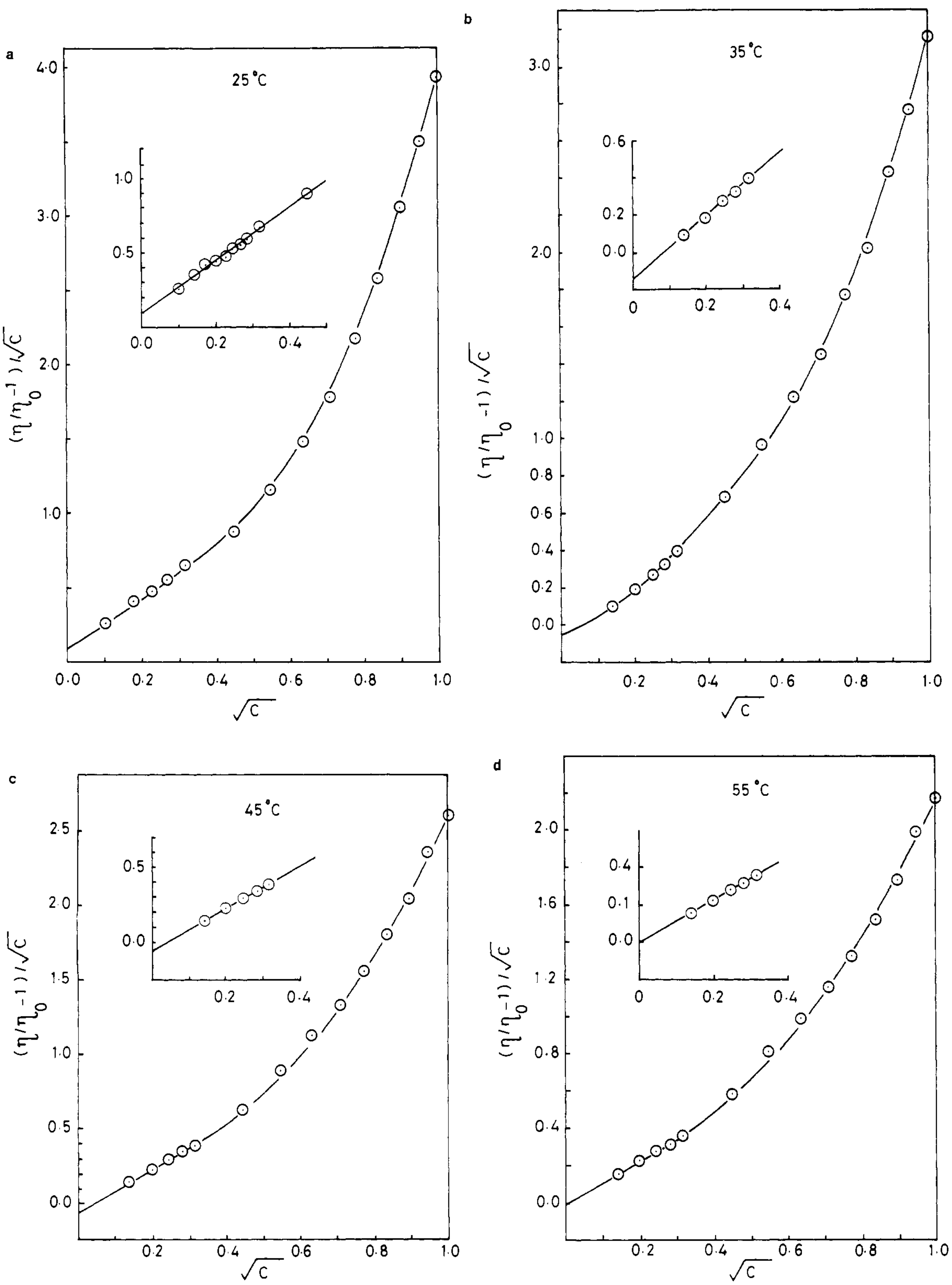

Figure 2. Plots of the variables $(\eta/\eta_0 - 1)/C^{1/2}$ versus $C^{1/2}$, at the temperatures (a) 25, (b) 35, (c) 45, and (d) 55 °C, for KI in NFM solutions.

negative one, producing an increase in the viscosity of the solution with respect to that of the NFM solvent, Figure 1.

In a comparison of the B coefficients for NFM in this work with that of other solvents published in the literature, such as dimethyl sulfoxide (DMSO) (*9*), hexamethylphosphorous triamide (HMPT) (*10*), methanol (MeOH) (*11*), ethylene glycol (EG) (*12*), Table II, the B coefficient decreases in the order NFM > HMPT > DMSO > MeOH > EG. This is probably due to the higher positive contribution to the B coefficient as a result of the tendency of KI to attract NFM molecules more than HMPT, DMSO, methanol, and EG.

Acknowledgment

We are indebted to Dr. Akl M. Awwad who generously provides his laboratory facilities and advice.

Glossary

A	Jones–Dole A coefficient
B	Jones–Dole B coefficient
C	concentration, mol/L
h	Planck's constant, m^2 kg s^{-1}
N	Avogadro's constant, mol^{-1}
R	molar gas constant, J K^{-1} mol^{-1}

T	temperature, K
$\bar{V}_1{}^\circ$	partial molar volume of the solvent, cm^3 mol^{-1}
$\bar{V}_2{}^\circ$	partial molar volume of the solute, cm^3 mol^{-1}
ρ	density, g cm^{-3}
η	absolute viscosity of solution, cP
η_0	absolute viscosity of pure solvent, cP
$\Delta\mu_1{}^{\circ\ddagger}$	free energy of activation per mole of the pure solvent, kJ mol^{-1}
$\Delta\mu_2{}^{\circ\ddagger}$	contribution per mole of the solute to the free energy of activation for viscous flow of the solution, kJ mol^{-1}

Registry No. NFM, 4394-85-8; KI, 7681-11-0.

Literature Cited

(1) Goldsack, D. E.; Franchetto, R. C. *Can. J. Chem.* **1977**, *55*, 1062.
(2) Goldsack, D. E.; Franchetto, R. C. *Can. J. Chem.* **1976**, *56*, 1442.
(3) Goldsack, D. E.; Franchetto, R. C. *Electrochim. Acta* **1977**, *22*, 1387.
(4) Desnoyers, J. E.; Perron, G. *J. Solution Chem.* **1972**, *1*, 199.
(5) Stein, M. *Hydrocarbon Processing* **1973**, *52*, 139.
(6) Cenelli, E.; Noe, S.; Paret, G. *Hydrocarbon Process.* **1972**, *51*, 141.
(7) Mueller, E.; Hoefeld, G. *Proc. World Pet. Congress, 8th* **1971**, *4*, 213.
(8) Jones, G.; Dole, M. *J. Am. Chem. Soc.* **1929**, *51*, 2950.
(9) Bicknell, R. T. M.; Lawrence, K. G.; Seeley, M. A.; Feakins, D.; Werblan, L. *J. Chem. Soc., Faraday Trans. 1* **1976**, *72*, 307.
(10) Sacco, A.; Petrella, G.; Della Monica, M.; Castagnolo. *J. Chem. Soc., Faraday Trans. 1* **1977**, *73*, 1936.
(11) Jones, G.; Fonwalt, H. J. *J. Am. Chem. Soc.* **1935**, *57*, 2041.
(12) Crickard, K.; Skinner, J. F. *J. Phys. Chem.* **1969**, *73*, 2060.
(13) Feakins, D.; Freemantle, D. J.; Lawrence, K. G. *J. Chem. Soc., Faraday Trans. 1* **1974**, *70*, 795.
(14) Glasstone, S.; Laidler, K. J.; Eyring, H. *The Theory of Rate Process*; McGraw-Hill: New York, 1941; p 477.

Received for review August 9, 1988. Revised May 9, 1989. Accepted October 2, 1989. We thank the Scientific Research Council for supporting this work.

Vapor–Liquid Equilibria at 1 atm for Binary and Ternary Systems Composed of Benzene, Toluene, and *m*-Xylene

Nurbay Gültekin

Faculty of Arts and Sciences, Karadeniz Technical University, Trabzon, Turkey

The vapor–liquid equilibrium data for the binary and ternary systems composed of benzene, toluene, and *m*-xylene at the isobaric condition of 1 atm are presented. The experimental data of the binary systems were used to calculate the binary parameters of the Wilson equation. The calculated vapor-phase compositions and boiling points of the three binary and of the ternary systems agree well with the experimental data.

Introduction

In continuation of our previous paper (*1*), we report now vapor–liquid equilibrium data at 1 atm of binary and ternary systems containing benzene, toluene, and *m*-xylene.

Benzene + toluene had been investigated previously by several authors (see ref 2). Isothermal data have been reported for benzene + *m*-xylene (see ref 2) or toluene + *m*-xylene (*3*). No data are available for the ternary system benzene + toluene + *m*-xylene.

Experimental Section

***Materials*.** The compounds used in this study were pure-grade materials obtained from E. Merck AG, Darmstadt, FRG. Their physical constants appear in Table I.

***Apparatus and* Procedure.** The apparatus has been described previously (*1*). The samples of vapor and liquid phases were analyzed by using a Perkin-Elmer Model 154-C gas chromatograph equipped with a Supelcowax 10 column (column temperature, 50–150 °C at 4 °C/min; flow rate, 5 mL/min of He (flow controlled)). The chromatograph was calibrated with gravimetrically prepared samples. The vapor-liquid equilibrium compositions were determined from the calibration curve with a linear interpolation technique (*4*) applied to related peak area composition data.

Table I. Pure Component Normal Boiling Points, T_b, and Refractive Indexes, n

	T_b (1 atm)/K		n_D (293.15 K)	
component	ref 16	measured	ref 16	measured
benzene	353.244	353.23	1.501 12	1.5008
toluene	383.780	383.73	1.496 78	1.4963
m-xylene	412.270	412.29	1.497 22	1.4978

Table II. Constants, C_i, of Modified Riedel's Equation (*5*, *6*) for the Pure Compounds Vapor Pressure, P_i, as Function of Temperature, T [a]

compound	C_1	C_2	C_3	C_4
benzene	978.622 633	−32 050.796 227	0.244 124	−166.030 37
toluene	85.415 932	−7 153.257 436	0.011 228	−11.946 659
m-xylene	72.700 426	−7 949.796 502	0.005 357	−9.421 028

[a] $\ln (P_i/\mathrm{atm}) = C_1 + C_2/(T/\mathrm{K}) + C_3(T/\mathrm{K}) + C_4 \ln (T/\mathrm{K})$.

The accuracies of x, y, P, and T are respectively 0.002, 0.002, 0.001 atm, and 0.1 K.

Experimental Results and Correlations

***Vapor Pressure*.** The vapor pressures of the three components have been calculated by using the modified Riedel equation (*5*). The constants of this equation were determined previously by Gültekin (*6*) for more than 1000 substances. These constants are shown in Table II.

***Binary Systems*.** The binary parameters λ_{ij} of the Wilson equation (*7*) were calculated from the related pure component data and the experimental results of the binary systems under consideration by using a simplex search method (*8*). Then, the vapor-phase compositions y_1 and boiling points T of the mixtures were calculated by using these parameters. The standard and mean deviations between experimental and calculated boiling points and vapor-phase compositions and the calculated activity coefficients γ_i for each binary system are given in Tables III–V. Vapor-phase nonideality has been taken into

0021-9568/90/1735-0130$02.50/0 © 1990 American Chemical Society